Environmental Science & Technology

pubs.acs.org/est

Article

Complex Mixture Analysis of Emerging Contaminants Generated from Coal Tar- and Petroleum-Derived Pavement Sealants: Molecular Compositions and Correlations with Toxicity Revealed by Fourier Transform Ion Cyclotron Resonance Mass Spectrometry

Taylor J. Glattke, Martha L. Chacón-Patiño, Sarajeen Saima Hoque, Thomas E. Ennis, Steve Greason, Alan G. Marshall,* and Ryan P. Rodgers*

Cite This: *Environ. Sci. Technol.* 2022, 56, 12988–12998

Read Online

ACCESS | Metrics & More | Article Recommendations | Supporting Information

ABSTRACT: Pavement sealants are of environmental concern because of their complex petroleum-based chemistry and potential toxicity. Specifically, coal tar-derived sealants contain high concentrations of toxic/carcinogenic polycyclic aromatic hydrocarbons (PAHs) that, when weathered, can be transferred into the surrounding environment. Previous studies have demonstrated the effects of coal tar sealants on PAH concentration in nearby waterways and their harmful effects in aquatic ecosystems. Here, we investigate and compare the molecular composition of two different pavement sealants, petroleum asphalt- and coal tar-derived, and their photoproducts, by positive-ion (+) atmospheric pressure photoionization (APPI) and negative-ion (−) electrospray ionization (ESI) coupled with ultrahigh-resolution Fourier transform ion cyclotron resonance mass spectrometry to address species (high-boiling and/or high oxygen content) that lie outside the analytical window of other techniques due to ultra-high molecular complexity. In addition, we evaluate the toxicity of the water-soluble photoproducts by use of Microtox bioassay. The results demonstrate that the coal tar sealant contains higher amounts of PAHs and produces abundant water-soluble compounds, relative to unweathered materials, with a high abundance of PAH-like molecules of high toxicity. By comparison, the asphalt sealant produces fewer toxic water-soluble species, with molecular compositions that are consistent with natural dissolved organic matter. These results capture the mass, chemical diversity, toxicity, and source/photoproduct relationship of these compositionally complex emerging contaminants from the built environment.

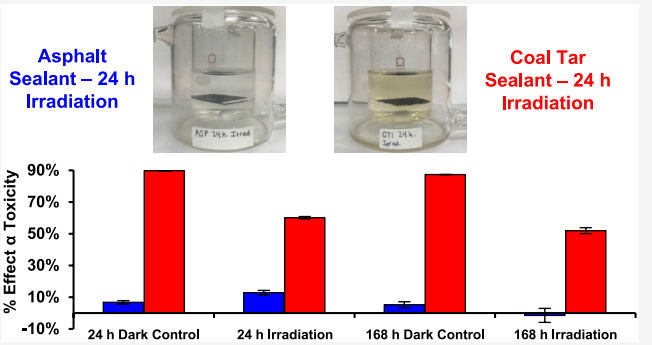

KEYWORDS: *Fourier transform mass spectrometry, ICR, FT-ICR, atmospheric pressure photoionization, electrospray ionization, polycyclic aromatic hydrocarbons, pavement, sealers*

INTRODUCTION

Photooxidation of Fossil Fuel-Derived Products. Fossil fuel-derived products such as crude oil and asphalt binder are known to produce highly oxidized oil- and water-soluble molecules upon weathering.[1−6] Previous works identify photooxidation by sunlight as a critical weathering process that transforms fossil fuels in the environment into oxidized photoproducts.[7−12] Various pathways have been suggested for the formation of oxidized water-soluble species from fossil fuel-derived products. For example, the work performed by Niles et al.[3] suggests that solar irradiation of asphalt binder, a common road paving material, yields polycyclic aromatic hydrocarbons (PAHs) with high oxygen content, by photo-induced oxidation and cracking reactions. These products can then undergo polymerization (addition reactions) to produce potentially toxic water-soluble compounds with higher oxygen content and increased carbon number, for example, molecules with up to 18 oxygen atoms and carbon number 35, relative to the oxidized products before polymerization. In another study, asphaltenes, a major component of crude oil distillation residues and therefore central for asphalt materials, were subjected to weathering in a solar simulator microcosm.[1,13] The results indicated a direct correlation between asphaltene molecular structure and their likelihood to produce water-soluble compounds. Specifically, it was concluded that samples with a high concentration of large, single aromatic cores (<7

Received: January 24, 2022
Revised: August 5, 2022
Accepted: August 5, 2022
Published: August 30, 2022

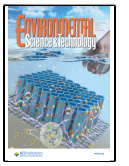

fused rings) leached limited amounts of water-soluble species. In contrast, samples enriched in smaller, multiple aromatic cores (<4 fused rings), interconnected by covalent bonds, were shown to produce abundant water-soluble molecules whose molecular composition resembled that of dissolved organic matter (DOM). These results implicate various characteristics of fossil fuel-derived products as being responsible for aiding production of water-soluble photoproducts when exposed to irradiation. Therefore, this finding suggests that similar photooxidation trends might be seen for other fossil fuel-derived products of widespread use in the built environment, such as pavement sealants and roofing materials.

Pavement Sealants. A sealant is a black, shiny emulsion that is sprayed or painted onto asphalt pavement in private roads and driveways, and business-owned/public parking lots to increase longevity of the pavement.[14] This product is marketed typically as a beautification and protection technique; however, its use can have harmful effects on wildlife and human health.[14] Two types of sealcoats are commonly used in the United States: coal tar emulsion sealant and asphalt emulsion sealant.[14] Coal tar sealants are composed of coal-derived products such as coal tar pitch, a distillation residue classified as a Group 1 human carcinogen by the International Agency of Research on Cancer (IARC),[15,16] that contains ∼200 known PAHs, which include naphthalene, anthracene, and benzo(*b*)thiophene.[14,17,18] Coal tar sealant is 15−35 wt % coal tar pitch, plus an emulsifying agent, water, sand, clay, and other additives.[19,20] Because it contains a high amount of coal tar pitch, the coal tar sealant, readily used in the eastern U.S., is enriched in PAHs.[14] Conversely, asphalt emulsion sealant, used mainly in the western U.S., is petroleum-based, comprised of petroleum distillation residues, and contains lower amounts of PAHs.[19] Sealcoats can undergo physical weathering by storm water runoff, tire-contact, snowplows, and general wear, and the coal tar sealant in particular can produce fine particles with high PAH concentrations.[21,22] These fine particles can be trapped in ponds, rivers, and streams, transported into larger water sources, and trapped in sediment where they can be photooxidized, yielding potentially toxic water-soluble species and subsequently increasing the PAH content in water.[14] For instance, Mahler et al. traced the concentration, as a function of time, of selected PAHs and azaarenes (N-substituted PAHs) in runoff from pavements coated with coal tar- and asphalt-based sealants.[23] Runoff from the coal tar-sealed pavement revealed disproportionally higher concentrations of known carcinogenic PAHs and azaarenes, for weeks to months following its application.[23] Specifically, the median concentration of 16 EPA Priority Pollutant PAHs in coal tar sealant runoff was ∼10-fold higher than that derived from the petroleum-based asphalt sealant.[23] Although physical weathering and subsequent contamination of waterways from the sealants due to general wear have been investigated, the chemical weathering and thus the molecular transformation of pavement sealants due to direct exposure to solar irradiation after application on road pavement and parking lots are still relatively unknown.

Environmental Contamination from Coal Tar Sealant. Evidence of contamination from weathering of coal tar sealant has been studied in various locations, such as Austin, Texas, U.S.A. and Minnesota, U.S.A., and has resulted in a ban of the use of this product in favor of alternative materials, such as asphalt emulsion or acrylic sealants.[20,24−26] Specifically, the work in Austin, Texas, has provided evidence for the PAH concentration in streambed sediments of creeks adjacent to large parking lots where coal tar sealant was used extensively.[25] In 2006, the city of Austin became the first to ban coal tar sealant and as a result, researchers saw an overall subsequent decline in the concentration of the 16 EPA Priority Pollutant PAHs in lake-collected sediment cores and bottom-sediment samples by approximately 58% from 2012−2014.[20] Furthermore, harmful effects on aquatic ecosystems and their inhabitants have been linked to high PAH concentrations from coal tar-based sources.[14,19,26] Various studies have revealed that leached PAHs from coal tar sealant, benzo(*a*)pyrene and benz(*a*)anthracene, are harmful to the overall health of the aquatic ecosystems, including, but not limited to, stunted development, liver problems, and death.[14]

To demonstrate the production of water-soluble contaminants from pavement sealants upon exposure to sunlight, we employ ultrahigh-resolution Fourier transform ion cyclotron resonance mass spectrometry (FT-ICR MS) to investigate and compare the molecular composition of the water-soluble molecules leached from two different types of sealant upon solar irradiation, that is, petroleum asphalt-based and coal tar-based products. FT-ICR MS enables molecular characterization of compounds in the sealants and their photoproducts, which are considered to be ultra-high complex mixtures that would otherwise be difficult to resolve with low-resolution MS techniques. The sealants, supplied as emulsions by Sitelab Corporation, were applied on glass slides, dried under nitrogen for 24 h (commercially suggested curing time), submerged in water, and irradiated in a solar simulator microcosm to mimic weathering in the environment. The oil-soluble photoproducts were separated from their water-soluble counterparts and analyzed by positive-ion (+) atmospheric pressure photoionization (APPI) and negative-ion (−) electrospray ionization (ESI) FT-ICR MS. The results indicate that the asphalt sealant generates photoproducts that resemble typical dissolved organic matter (DOM) seen previously for other petroleum-based products. Conversely, photoproducts from the coal tar sealant are PAH-like and present higher toxicity than asphalt sealant. These results provide a basis for future work: namely, how PAH assemblages change in the hours to days after the application of sealant in a real-world setting. From an environmental standpoint, these low molecular weight (LMW) PAHs, such as the above-mentioned benzo(*a*)pyrene and benz(*a*)anthracene, have chemical characteristics and ecotoxicological properties different from those of high molecular weight PAHs.[27]

EXPERIMENTAL METHODS

Pavement Sealants. Two different pavement sealants, petroleum asphalt sealant and coal tar sealant, were obtained from Sitelab Corporation (West Newbury, MA, U.S.A). The samples were provided as ready-to-use products, which contained emulsions of asphalt or coal tar mixed with water and other additives, and were stored in the dark. Both sealants are classified as Type 1 and have known PAH concentrations. The asphalt sealant has an EPA Priority PAH concentration of less than 50 ppm and the coal tar sealant contains between 50 000 and 75 000 ppm as measured by the EPA method 8270D-SIM.[28]

Photooxidation of Pavement Sealants in a Solar Simulator Microcosm. Films of pavement sealant were prepared by spreading the emulsions, as they were received,

https://doi.org/10.1021/acs.est.2c00582
Environ. Sci. Technol. 2022, 56, 12988−12998

onto a glass slide. All glassware used was cleaned and combusted at 550 °C in a muffle furnace to remove any organic carbon prior to irradiation. The layer of sealant was dried under nitrogen, and additional layers were added until a mass of 300 mg was obtained. Once fully dry (~24 h), the slide with the film was placed in a jacketed beaker, coupled to a water chiller at 27 °C, on a glass ring to enable a stir bar to sit underneath the glass slide (Figure S1). The sealant film was submerged in 50 mL of deionized water (HPLC-grade, J.T. Baker, Philipsburg, NJ). The prepared jacketed beaker was placed in an ATLAS Suntest CPS solar simulator (300−800 nm, 250−765 W/m^2 irradiance range, 1500 W Xenon lamp)[10] and irradiated for either 24 h or 168 h, with magnetic stirring (100 rpm). The periods of irradiation are equivalent to approximately 6 and 42 days of exposure to natural sunlight in Gulf of Mexico conditions.[29] Dark controls were prepared similarly, covered with aluminum foil, and allowed to stir for the same time periods. After irradiation, all water was removed with a Pasteur pipet, transferred to a clean/muffled glass vial, and stored in the dark at approximately 3.3 °C to prevent further oxidation. The irradiated sealant (oil-solubles) was removed from the glass slide by dissolution in toluene (HPLC-grade, J.T. Baker, Philipsburg, NJ) assisted by sonication (Branson Ultrasonics, Danbury, CT, 22 kHz, 130 W), dried under nitrogen, and stored in the dark for subsequent molecular-level characterization.

Molecular-Level Characterization by 9.4 T FT-ICR MS. Stock solutions of the starting and irradiated pavement sealants were prepared in toluene at a concentration of 10 mg/mL and further diluted to 100 μg/mL for analysis by (+) APPI coupled with a custom-built 9.4 T FT-ICR mass spectrometer.[30−32] The samples were directly infused at 50 μL/min into an Ion Max APPI source (Thermo Fisher Scientific, Waltham, MA, U.S.A.) at a vaporizer temperature of 320 °C. Gas-phase neutrals were photoionized with 10.2 eV photons from an ultraviolet krypton lamp (Syagen Technology Inc., Tustin, CA, U.S.A). Positive ions were transferred into the mass spectrometer via a heated metal capillary (~350 °C) and analyzed with a dynamically harmonized ICR cell.[33,34] Approximately 5 mL of the collected water-solubles were completely dried under nitrogen and diluted with methanol (HPLC-grade, J.T. Baker, Philipsburg, NJ) to a concentration of 400 μg/mL. The samples were directly infused into the mass spectrometer via a heated metal capillary by use of (−) microelectrospray ionization (ESI) at a flow rate of 0.5 μL/min. For each spectrum, 150 time-domain transients were co-added.[35] Custom Predator and PetroOrg© Software enabled data collection, Fourier transformation, phasing, mass spectral calibration, molecular formula assignment, and data visualization.[35−37]

Dissolved Organic Carbon Analysis of Water-solubles. Dissolved organic carbon (DOC) concentrations were measured with a Shimadzu (Columbia, MD, U.S.A.) total organic carbon (TOC-V WS) analyzer. Each water sample was diluted with deionized water (10 mL sample + 30 mL deionized water). Samples were acidified to pH 2 with phosphoric acid (H_3PO_4), and the acid injection in each sample was 3%. 1.5% of sodium persulfate was injected as the UV oxidizing agent. The sample concentrations were determined with a six-point calibration curve between 0 and 50 ppm (0, 1, 5, 10, 20, and 50 ppm) from a laboratory-prepared 1000 ppm organic carbon stock solution, which consisted of potassium hydrogen phthalate and deionized water. No blank injections were run between each sample injection. To ensure that the samples were within the calibration range, the auto-dilution feature on the TOC analyzer was enabled. The acidified samples (pH 2) were sparged for 3 min. The mean of three injections of 6 mL was reported for every sample, and the coefficient of variance was 2% for replicate injections.

Microtox Bioassay Screening of Water-solubles. The Microtox 40% screening test procedure (Microtox model 500 analyzer, Modern Water, New Castle, DE) was performed to test the acute toxicity of the leached water-soluble species by inhibition of *Aliivibrio fischeri* bioluminescence.[38] The water-soluble samples from the irradiations and dark controls were carbon-normalized with deionized water to dilute all samples to the lowest DOC concentration result (7.73 mg/mL), measured from the above-mentioned DOC procedure. This procedure enables toxicity to be measured relative to sample composition, rather than absolute concentration. The samples were prepared for the screening test according to manufacturer's instructions (incubated, diluted with 2% sodium chloride (NaCl) solution, and modified with 22% NaCl osmotic solution to adjust salinity) and analyzed. The emission of light from *A. fischeri* bioluminescent bacteria (490 nm) added to the water samples was measured relative to a blank sample and reported as percent effect (% effect).

RESULTS AND DISCUSSION

Molecular Composition of the Starting Material. To gain insight about how the different sealants respond to weathering in the environment, the molecular compositions of the starting material (i.e., unirradiated sealants) were analyzed by direct infusion (+) APPI FT-ICR MS. Analysis of the whole asphalt and coal tar sealants revealed remarkable differences between the samples. The thousands of peaks detected in the mass spectra of the samples were calibrated with internal homologous Kendrick series,[39] and each assigned a unique molecular formula ($C_cH_hN_nO_oS_s$). The molecular formulas are sorted according to their heteroatom content; for instance, all formulas with only carbon and hydrogen comprise the hydrocarbon class (HC);[40] whereas species with C, H, and one S atom make up the S_1 class. Knowledge of the molecular formulas enables the calculation of double bond equivalents (number of rings plus double bonds to carbon), calculated with the equation,[41] DBE = c − h/2 + n/2 + 1, which represents a measure of a compound's aromaticity. Figure 1 displays the heteroatom class distribution (top) and iso-abundance-contoured plots of double bond equivalents (DBE) versus carbon number (bottom), in which the color scale represents relative abundance (RA). Compounds with equal DBE but varying degrees of carbon number (or CH_2 units) belong to the same homologous series. Previous work by Bowman et al.[42] utilized two-dimensional gas chromatography-high-resolution mass spectrometry (GC × GC/HRMS) to analyze coal tar and asphalt sealant and assigned 88 and 337 unique elemental compositions. By comparison, our analysis with ultrahigh-resolution FT-ICR MS enabled the assignment of 2290 and 12191 monoisotopic molecular formulas in coal tar and asphalt sealant, a significant improvement in compound accessibility and assignment because APPI can volatize and ionize high-boiling point/heteroatom-containing compounds which are not accessible and/or resolved by routinely used GC-based MS techniques. The unirradiated whole samples present high abundances of hydrocarbon (HC) and nitrogen

https://doi.org/10.1021/acs.est.2c00582
Environ. Sci. Technol. 2022, 56, 12988−12998

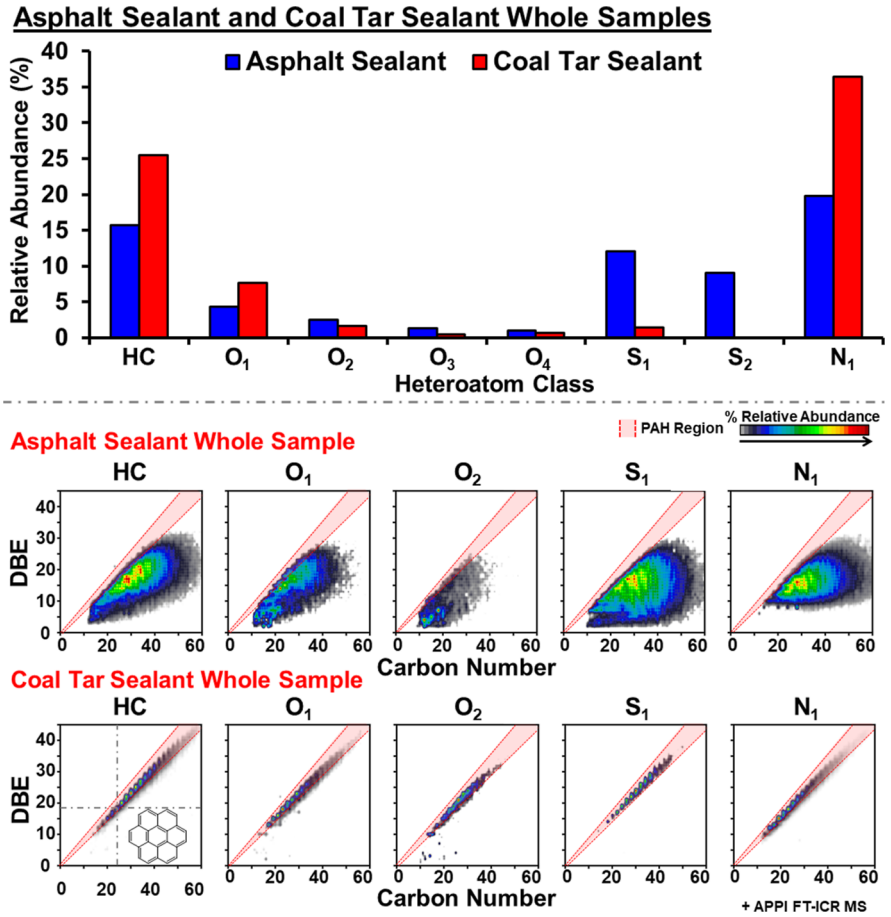

Figure 1. Heteroatom class distribution (top panel) and isoabundance color-contoured plots of double bond equivalents (DBE) versus carbon number (bottom panel) derived from (+) APPI 9.4 T FT-ICR MS for the most abundant heteroatom classes from the analysis of asphalt sealant (blue) and coal tar sealant (red) starting material.

(N_1) species, above 15% RA. Asphalt sealant contains high amounts of sulfur species (~21% RA), which is consistent with distillation residues from heavy petroleum.[43] Conversely, coal tar sealant contains a higher total abundance of oxygen-containing species (O_{1-4} classes), ~10% RA, and almost 37% of N_1 compounds. This result is expected because coal tar sealant is derived from raw coal and its byproducts which are known to be highly oxygenated and comprise high amounts of nitrogen-containing aromatic cores (azaarenes).[44−49] The lack of sulfur in the coal tar sealant is also expected because sulfur is released, as H_2S, during pyrolysis of coal.[50,51] The heteroatom content also suggests that upon photooxidation, the irradiated coal tar sealant will be abundant in O_x and NO_x classes; whereas, asphalt sealant products will likely be more abundant in SO_x compounds. Moreover, the bottom panel of Figure 1 reveals that the compositional ranges of the two sealants are drastically different. Coal tar sealant extends to higher DBE values (~10 − 45), which indicates higher content of highly aromatic compounds, likely with up to ~16 fused aromatic rings. For reference, the structure of coronene (7-rings, carbon number = 24, DBE = 19) has been included in the DBE versus carbon number plot for the HC class. In addition, coal tar sealant features a compositional range with short homologous series (low levels of alkylation), species with the same DBE but varying carbon number: it contains almost-discrete abundant series (green-yellow/red spots) with short carbon number ranges for each DBE value that lies within the PAH region (red highlighted region). This PAH region consists of the area between two compositional boundaries: the planar PAH limit and the catacondensed PAH limit. The planar PAH limit is a compositional boundary for naturally occurring fossil hydrocarbons and indicates that the DBE value of planar petroleum molecules should not exceed ~90% of its carbon content. DBE values above this limit indicate the presence of fullerene-type compounds, which are not naturally present in fossil fuels.[52] The catacondensed PAH limit indicates the region at which catacondensed PAHs would be present (DBE = 0.75C − 0.5).[53−55] Conversely, species located to the far right are highly alkyl-substituted and less condensed. Thus, molecules with DBE values closer to 90% of their carbon number are alkyl-deficient, pericondensed PAHs (which contain several carbon atoms shared by more than two aromatic rings).[56] In contrast, the asphalt sealant compositional range features DBEs below 30 and extended homologous series, which indicates a high abundance of less aromatic/alkyl-enriched compounds.

The results indicate that the coal tar sealant starting material is enriched in near bare PAHs of environmental concern such as, naphthalene, pyrene, and benzo(*a*)pyrene, among others (shown in Figure S2). These PAHs are known to be carcinogenic and have been included as harmful contaminants on the EPA Priority Pollutant List.[57] In contrast, asphalt sealant comprises continuous series that occupy carbon number ranges between 10 and 60 and below DBE 30. For instance, the DBE versus carbon number plot for the S_1 class

https://doi.org/10.1021/acs.est.2c00582
Environ. Sci. Technol. 2022, 56, 12988−12998

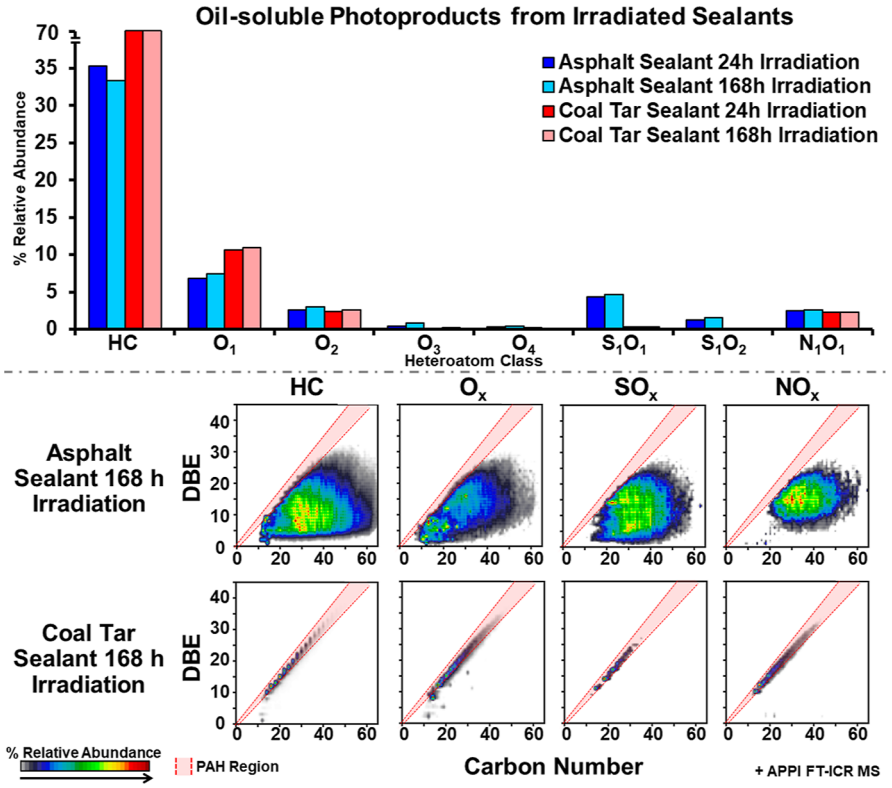

Figure 2. Heteroatom class distribution (top panel) and isoabundance color-contoured plots of DBE versus carbon number (bottom panel) for the most abundant oil-soluble species' oxidized heteroatom classes derived from (+) APPI 9.4 T FT-ICR MS analysis of the 24 h and 168 h irradiations of the asphalt sealant (blue shades) and coal tar sealant (red shades).

suggests the presence of an extended homologous series at DBE = 6 and carbon numbers between 10 and 55, which suggests abundant benzothiophene rings (DBE 6) with up to ~45 carbon atoms in alkyl-side chains (CH_2 units). The differences in molecular composition between asphalt and coal tar sealants suggest that upon photooxidation, the coal tar sealant will likely produce oil- and water-soluble photoproducts with molecular compositions near the PAH line (low alkylation). Conversely, the asphalt sealant will produce oil- and water-soluble species with various degrees of alkylation, similar to other petroleum-based products.[3,58−60]

Photooxidation of Pavement Sealants. Films of coal/asphalt sealants were irradiated in a solar simulator microcosm to mimic weathering in the environment. After irradiation of the two pavement sealants for two different time periods (24 h and 168 h), (+) APPI FT-ICR MS was used to analyze the oil-soluble photoproducts. The most abundant heteroatom classes (RA > 1%) identified in the oil-soluble species are displayed in the upper panel of Figure 2. The compositions for only the 168 h irradiation are displayed in the bottom panel because there were no significant differences between the oil-soluble products for their respective 24 and 168 h time periods in both irradiations and dark controls (Figure S3). Compared to the starting material, both irradiated sealants contain a higher abundance of oxidized species, O_x and NO_x. In particular, the asphalt sealant reveals higher amounts of SO_x species, as expected based on the analysis of the starting material (high sulfur content). Furthermore, the abundance of the HC class, in both sealants, increased upon irradiation: the coal tar sealant increased from 25.5% RA to 70% RA and asphalt sealant increased from 15% RA to ~35% RA. That increase suggests that heteroatoms are potentially contained in labile moieties connected to hydrocarbon cores, such as side chains, which are released by photochemical reactions, and potentially transformed into water-soluble compounds. Upon photooxidation, these moieties can crack off the structure, which leaves behind the hydrocarbon core. Compositionally, the two irradiated sealants demonstrate results similar to their respective starting materials. The irradiated asphalt sealant contains continuous series that occupy low DBE (DBE < 30) and carbon number (10−60) range. The coal tar sealant oil-soluble photoproducts reveal "discrete" abundant series between carbon numbers 10 and 40 and up to DBE 35, which is a slight decrease in aromaticity compared to the starting material. Moreover, the irradiated compounds remain along the PAH limit line, suggesting the continued presence of PAHs after photooxidation (Figure S1).

In addition to the characterization of the oil-soluble photoproducts, the water-soluble species produced from the irradiations and dark controls of the sealants were analyzed by (−) ESI FT-ICR MS, which targets polar/acidic species, known to form through the photooxidation of hydrocarbons.[59] ESI has been used to access the molecular composition of the water-soluble photoproducts because it enables more uniform ionization for that type of sample than APPI.[1] Thus, it is widely reported that (−) ESI FT-ICR MS is well suited for the characterization of petroleum-derived DOM.[59,61−63] Figure 3 shows the relative abundances and combined compositional range for O_x (top) and NO_x (bottom) classes detected in the water samples upon simulated solar irradiation. O_x water-soluble compounds from the asphalt sealant contain up to ten oxygen atoms (O_{10} class), with higher abundances for compounds with low oxygen number (O_2−O_5). The coal tar sealant water-soluble products contain up to the O_{12} class and

https://doi.org/10.1021/acs.est.2c00582
Environ. Sci. Technol. 2022, 56, 12988−12998

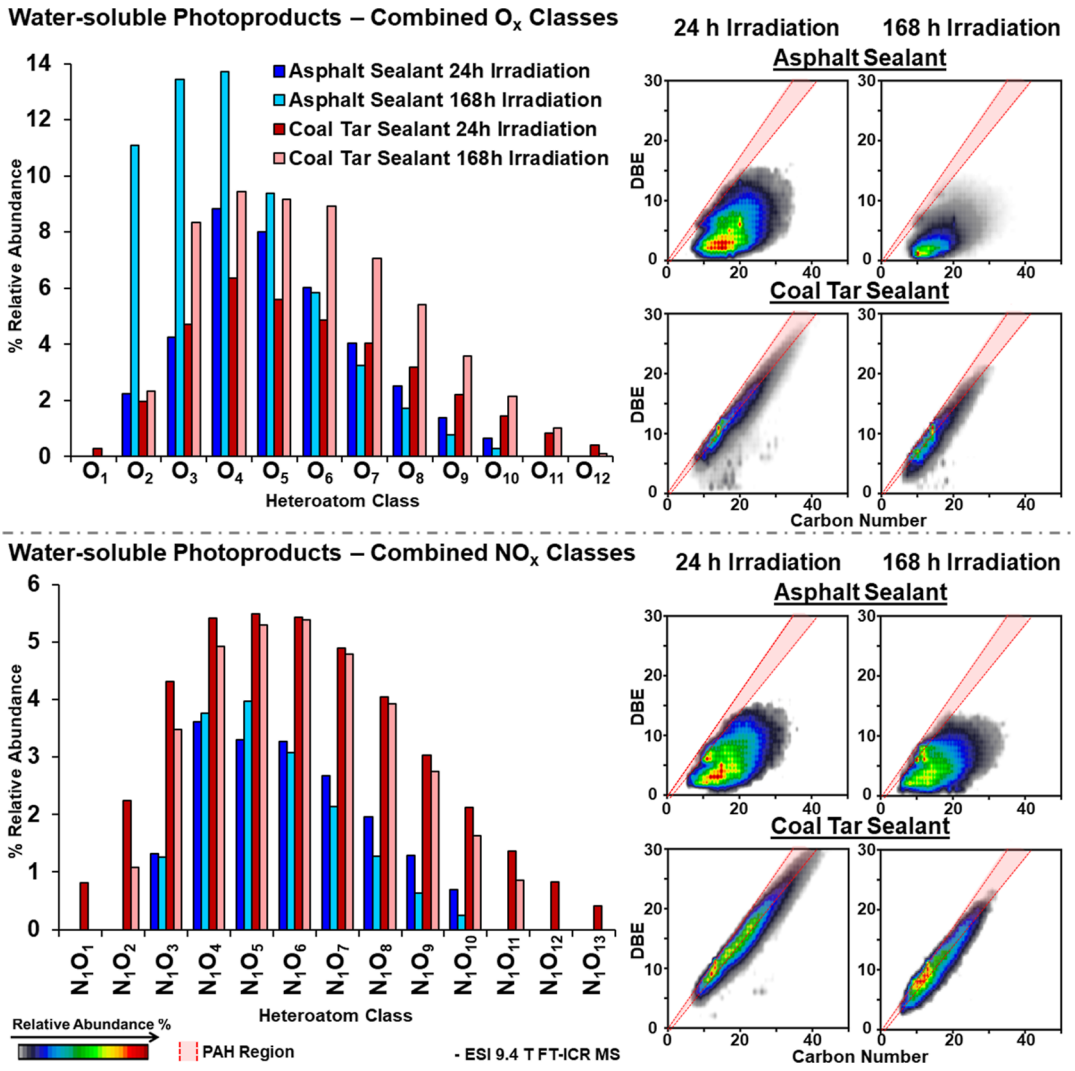

Figure 3. Heteroatom class distributions (left) and isoabundance color-contoured plots of DBE versus carbon number (right) for combined O_x (top panel) and NO_x (bottom panel) water-soluble species derived from (−) ESI 9.4 T FT-ICR MS analysis of the 24 h and 168 h irradiation periods from asphalt sealant (blue shades) and coal tar sealant (red shades).

are enriched in O_4−O_6 species. For both sealants, the abundance of oxygen increases with irradiation period. For N-containing water-soluble products, the coal tar sealant contains much higher abundances of NO_x classes (up to NO_{13}) than the asphalt sealant (up to NO_{10}). That result is expected based on the characterization of the starting materials, which confirmed a higher abundance of nitrogen-containing compounds for coal tar sealant. Furthermore, the compositional ranges of the water-soluble species for both O_x and NO_x combined classes follow expected trends deduced from the molecular composition of the starting material and irradiated oil-soluble compounds. The asphalt sealant water-soluble species exhibit a low DBE range (DBE < 15) and extended homologous series with up to ∼25 CH_2 units (carbon atoms), indicating a higher degree of alkylation and lower aromaticity than the coal tar products. The compositions of the water-soluble species from the asphalt sealant can also be compared to the respective oil-soluble species, which have more extended homologous series. The length of a homologous series increases from the addition of nonpolar CH_2 units; thus, asphalt-derived oil-soluble products have higher hydrophobicity. In addition, the compositions of the photogenerated water-soluble species from the asphalt sealant resemble trends seen for typical DOM from other fossil fuel-based products,[3,10] but at lower DBE values.

Coal tar sealant water-soluble species feature higher DBE (up to DBE 30) with carbon numbers up to 40. However, the homologous series are narrower than for asphalt water-soluble photoproducts. Furthermore, the photoproducts lie along the PAH limit line, suggesting that PAHs, originally present in the starting material, were able to move into the water upon photooxidation. Comparison of the compositional range of the water-soluble products and the oil-soluble species (coal tar starting material and oil-soluble photoproducts, Figures 1 and 2) indicates that the water-soluble compounds do not contain the defined/discrete homologous series with particular DBE values and instead, feature a continuous compositional range. This outcome suggests that photochemical reactions can cause structural changes that affect the DBE. For instance, photo-oxidation may cause oxygen incorporation as ketones, aldehydes, or carboxylic acids. It is important to note that it is difficult to make definitive conclusions about the molecular composition of water-soluble photoproducts because of the wide range of ionization efficiencies in (−) ESI, inherent to the

https://doi.org/10.1021/acs.est.2c00582
Environ. Sci. Technol. 2022, 56, 12988−12998

tens-of-thousands of different molecules in the samples. (−) ESI targets acidic species, which ionize more efficiently than compounds with no acidic functionalities. Moreover, less hydrophobic acids (low carbon number) ionize much more efficiently via ESI than higher carbon number acidic species.[64] Therefore, it is possible that the DBE versus carbon number plots in Figure 3 do not completely represent the composition of the water-soluble products. To see species difficult to ionize by (−) ESI, extensive fractionation of the water-soluble species is required, the topic of a future manuscript. For the purpose of this work, conclusions about the composition of the whole/unfractionated water-soluble sample are discussed.

The SO_x classes for the water-soluble species were also analyzed (Figure S4); however, the low abundance of sulfur in the coal tar starting material resulted in few or no SO_x species detected in the recovered water-solubles. Moreover, the few coal tar sulfur species consist of DBE values ≥ 3, suggesting the presence of thiophenic functionalities (i.e., sulfur contained in aromatic cores).[65,66] However, the asphalt sealant does contain abundant SO_x species (up to SO_{11} for 168 h irradiation), which exhibit a compositional range relative to the O_x and NO_x classes (DBE below 15, carbon number 5−30). Furthermore, asphalt water-soluble sulfur species reveal abundant low DBE compounds (<3 DBE), suggesting that sulfur is present (with oxygen) as sulfides and/or sulfoxides (−S═O).[66]

The compositions of the water-soluble photoproducts recovered from the dark controls are shown in Figures S5 and S6. The water from most of the dark controls shows little to no definitive compositional trends. Conversely, the O_x heteroatom group of the coal tar sealant 24 h dark control reveals a considerable abundance of oxygen (up to O_{14}) and compositions that lie along the PAH limit line. The high abundance of originally water-soluble oxygen-containing compounds, which are leached into the water without irradiation, can result from the processing of raw coal to produce coal tar pitch during the pyrolysis of coal and coal tar.[67,68] It is possible that water-soluble species from coal tar sealant are easily transferred into water without exposure to irradiation due to the presence of the emulsifying agent (characteristic of commercially available sealant emulsions). However, these species are not detected in (+) APPI analysis of the whole starting material, likely because of their much lower concentration than HC/N_1 compounds and more efficient ionization of highly aromatic (DBE > 15)/pericondensed aromatic cores. In contrast, the asphalt dark control water-soluble species present a non-continuous compositional range, which can be associated with background chemical noise captured during MS analysis, indicating that minimal water-soluble species are present. Furthermore, the number of monoisotopic molecular formulas for the dark controls can be compared to the irradiated samples to highlight the diversity of species that were generated during photooxidation. For example, for the 24 h dark controls, 665 and 2,400 molecular formulas were assigned for the asphalt and coal tar sealants; whereas for the 24 h irradiation, 8427 and 7596 were assigned. The increase in molecular formulas was also seen for the 168 h irradiation period: 1778 formulas for the dark control increased to 6936 for asphalt sealant, and 1315 formulas for the dark control increased to 2711 for coal tar sealant, indicating that upon photooxidation, more newly formed water-soluble species are generated. The presence of newly formed water-solubles is also supported by the reduced compositional ranges seen for the dark control samples relative to the irradiated samples. It should be pointed out that complex mixtures suffer from selective ionization; however, when sample sets are analyzed under the same conditions, the accessed compositional trends, via MS, can be useful to understand chemical processes, such as photooxidation. With APPI, PAHs typically have higher ionization efficiencies due to lower ionization potentials; whereas, in (−) ESI, there is efficient ionization of oxygen-containing acidic species of LMW.[64]

Quantification of Total Organic Carbon Leached from Pavement Sealants. In addition to molecular-level analysis, the amount of organics that were leached from the pavement sealants into the water was quantified by DOC measurements. Figure 4 displays the amount of DOC leached into the water from the irradiated and dark control asphalt (blue) and coal tar (red) samples. For both sealants, the amount of DOC increased upon photoirradiation. For example, the 168 h irradiated coal tar sealant produced nearly three times the amount of DOC than the 168 h dark control. The highest amount of DOC, ∼65.09 mg/L, was produced by 168 h irradiation of the asphalt sealant; whereas the same irradiation period for the coal tar sealant produced only approximately half that amount, ∼31.99 mg/L. In addition, both the 24 h and 168 h dark controls produced more DOC than has been seen previously for dark controls of other fossil fuel-based products.[3] The DOC results from the dark controls suggest that there are compounds in the sealants that can easily transfer into water without exposure to solar irradiation. These water-soluble compounds could potentially be attributed to the emulsifying agent that is added to the sealant for its application in the built environment. Therefore, it is important to understand how the coal tar sealant behaves, under solar irradiation, without the presence of the initial water-soluble compounds. To that end, a 24 h dark control for the coal tar sealant was prepared and the water-soluble species were collected. The remaining sealant on the glass slide was submerged in a fresh aliquot of water and subsequently irradiated for 24 h. This "washed" sample was separated and analyzed in the same manner as previously discussed (Figure S7), which included DOC analysis (Figure 4, right). The resulting DOC measurement for the washed coal tar sample was approximately 68 mg/L, which is ∼2× higher than

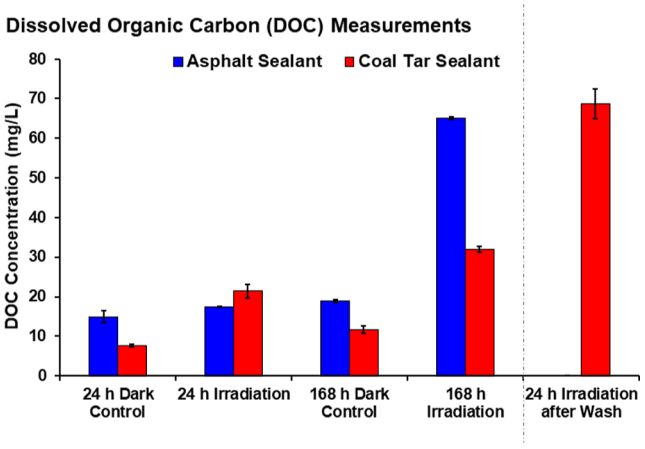

Figure 4. DOC measurements for water collected after 24 h and 168 h dark controls and irradiations of asphalt sealant (blue) and coal tar sealant (red).

https://doi.org/10.1021/acs.est.2c00582
Environ. Sci. Technol. 2022, 56, 12988−12998

observed for the 24 h irradiation experiment that contains the initial water-soluble compounds and photoproducts. This finding strongly suggests that the initial weathering process (water washing) affects the amount of leachable photoproducts with subsequent photoirradiation. Future research will aim to understand this behavior further.

The molecular composition of the water-soluble species for the 24 h washed coal tar sample is somewhat similar to that of the 24 h initial irradiation (unwashed). As previously discussed, the unwashed sample contains up to O_{12} and NO_{13}; whereas, the washed sample contains up to O_{11} and NO_{11}. However, the washed sample contains a higher total amount of O_x species (~53% RA) than the unwashed sample (~36% RA). For the NO_x species, the unwashed sample contains a slightly higher total amount (~40% RA) than the washed sample (~32% RA). The unwashed sample occupies slightly higher DBE ranges (up to DBE 30) than the washed sample for both the O_x and NO_x classes. Both compositional ranges lie along the PAH limit line, demonstrating that PAH-like compounds were still transferred into the water upon photoirradiation, despite the wash beforehand.

Toxicity of Water-solubles Determined by Microtox Bioassay. All water-soluble samples were subjected to Microtox bioassay analysis to determine acute toxicity of the water-soluble compounds produced from the sealant. In Figure 5, the percent effect (*y*-axis) on the bioluminescence is directly correlated to the toxicity of the sample: the higher the percent effect, the higher the toxicity of the sample. It is evident from Figure 5 that the coal tar sealant is more acutely toxic than the asphalt sealant, which shows little to no toxic effects. Both coal tar dark controls exhibit the highest toxicity readings (~90%), and the irradiated coal tar samples were also high in toxicity, but lower relative to the dark controls (between 50 and 60%): trends seen previously for DOM samples in which exposure to photooxidation over time decreased their toxicity.[69] Due to the high toxicity of the coal tar dark controls, the toxicity of the "washed" sample was also measured at approximately 15% effect, a drastic decrease from the irradiated coal tar sample. That decrease suggests that the compounds that are initially water-soluble before irradiation are the main source of the high toxicity in the coal tar sealant. It is concerning that these compounds are readily transferred to the aqueous phase, even after following the recommended curing time: 24 h drying prior to exposure to, for example, rain, traffic (in our case, contact with water). These toxic compounds could potentially be the parent PAHs that are easily transferred to the water and kept solvated by the emulsifying agent.[70] Once parent PAHs have contaminated waterways, they are difficult to completely remove and can be further exposed to weathering effects such as solar irradiation.[71] Thus, it is important to consider the contribution to toxicity from the formation of oxidized PAHs (oxy-PAHs) after photooxidation. Previous studies have reported that oxy-PAHs pose a threat to humans and the environment; and although their toxic effects may not be as detrimental as their parent PAHs, they should still be taken into consideration as important contaminants due to their persistence and increased mobility in the environment.[71] Note that the present toxicity test is applicable to compare the potential effects the sealants would have in a groundwater environment and the species living within them.[72−74] Toxic effects on human cell lines require additional testing that will be explored in future work.

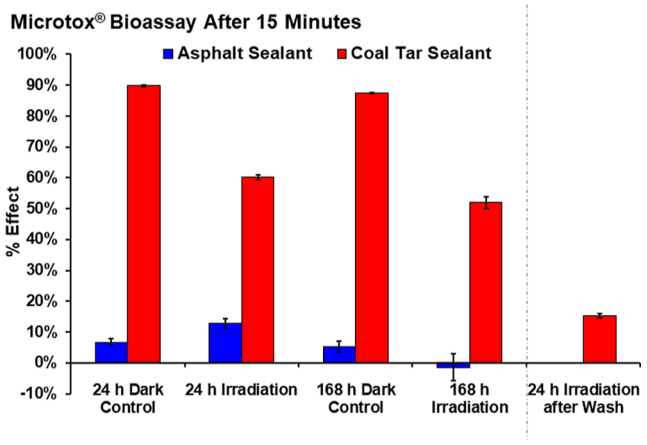

Figure 5. Percent effect (% effect) measurements due to the inhibition of emitted light from bioluminescent bacteria after 15 min, acquired from Microtox bioassay for water samples collected after 24 h and 168 h dark controls and irradiations of asphalt sealant (blue) and coal tar sealant (red).

■ ASSOCIATED CONTENT

Supporting Information

The Supporting Information is available free of charge at https://pubs.acs.org/doi/10.1021/acs.est.2c00582.

Experimental setup for solar simulator microcosm experiments; PAHs assigned in the HC class of coal tar sealant starting material and after irradiation; isoabundance color-contoured plots of DBE versus carbon number for (+) APPI FT-ICR MS analysis of the 24 h irradiations and dark control oil-solubles for the asphalt and coal tar sealants; heteroatom class distributions, RAs, and isoabundance color-contoured plots of DBE versus carbon number for SO_x classes in irradiated sealants and O_x, NO_x, and SO_x classes in the dark controls from (−) ESI FT-ICR MS analysis of asphalt and coal tar sealants; and heteroatom compound class distribution and isoabundance color-contoured plots of DBE versus carbon number for the washed coal tar sample (PDF)

■ AUTHOR INFORMATION

Corresponding Authors

Alan G. Marshall − *Ion Cyclotron Resonance Program, National High Magnetic Field Laboratory, Florida State University, Tallahassee, Florida 32310, United States; Department of Chemistry and Biochemistry, Florida State University, Tallahassee, Florida 32308, United States;* orcid.org/0000-0001-9375-2532; Phone: +1 850-644-0529; Email: marshall@magnet.fsu.edu; Fax: +1 850-644-1366

Ryan P. Rodgers − *Ion Cyclotron Resonance Program, National High Magnetic Field Laboratory, Florida State University, Tallahassee, Florida 32310, United States; Department of Chemistry and Biochemistry, Florida State University, Tallahassee, Florida 32308, United States;* orcid.org/0000-0003-1302-2850; Phone: +1 850-644-2398; Email: rodgers@magnet.fsu.edu; Fax: +1 850-644-1366

Authors

Taylor J. Glattke − *Ion Cyclotron Resonance Program, National High Magnetic Field Laboratory, Florida State University, Tallahassee, Florida 32310, United States; Department of Chemistry and Biochemistry, Florida State University, Tallahassee, Florida 32308, United States;* orcid.org/0000-0003-2934-0749

Martha L. Chacón-Patiño − *Ion Cyclotron Resonance Program, National High Magnetic Field Laboratory, Florida State University, Tallahassee, Florida 32310, United States;* orcid.org/0000-0002-7273-5343

Sarajeen Saima Hoque − *Department of Civil & Environmental Engineering, FAMU-FSU College of Engineering, Florida State University, Tallahassee, Florida 32310, United States*

Thomas E. Ennis − *Watershed Protection Department, City of Austin, Austin, Texas 78767, United States*

Steve Greason − *Sitelab Corporation, West Newbury, Massachusetts 01985, United States*

Complete contact information is available at: https://pubs.acs.org/10.1021/acs.est.2c00582

Notes

The authors declare no competing financial interest.

■ ACKNOWLEDGMENTS

A portion of this work was performed at the National High Magnetic Field Laboratory ICR User Facility, which is supported by the National Science Foundation Division of Chemistry through Cooperative agreement no. DMR-1644779 and the State of Florida. The authors thank Huan Chen for assistance with the performance of the Microtox bioassay experiments.

■ REFERENCES

(1) Chacón-Patiño, M. L.; Niles, S. F.; Marshall, A. G.; Hendrickson, C. L.; Rodgers, R. P. Role of Molecular Structure in the Production of Water-Soluble Species by Photo-oxidation of Petroleum. *Environ. Sci. Technol.* **2020**, *54*, 9968−9979.

(2) Zito, P.; Podgorski, D. C.; Bartges, T.; Guillemette, F.; Roebuck, J. A.; Spencer, R. G. M.; Rodgers, R. P.; Tarr, M. A. Sunlight-Induced Molecular Progression of Oil into Oxidized Oil Soluble Species, Interfacial Material, and Dissolved Organic Matter. *Energy Fuels* **2020**, *34*, 4721−4726.

(3) Niles, S. F.; Chacón-Patiño, M. L. S. P.; Putnam, R. P.; Rodgers, A. G.; Marshall, A. G. Characterization of an Asphalt Binder and Photoproducts by Fourier Transform Ion Cyclotron Resonance Mass Spectrometry Reveals Abundant Water-Soluble Hydrocarbons. *Environ. Sci. Technol.* **2020**, *54*, 8830−8836.

(4) Aeppli, C.; Carmichael, C. A.; Nelson, R. K.; Lemkau, K. L.; Graham, W. M.; Redmond, M. C.; Valentine, D. L.; Reddy, C. M. Oil Weathering after the Deepwater Horizon Disaster Led to the Formation of Oxygenated Residues. *Environ. Sci. Technol.* **2012**, *46*, 8799−8807.

(5) Maki, H.; Sasaki, T.; Harayama, S. Photo-Oxidation of Biodegraded Crude Oil and Toxicity of the Photo-Oxidized Products. *Chemosphere* **2001**, *44*, 1145−1151.

(6) Charrié-Duhaut, A.; Lemoine, S.; Adam, P.; Connan, J.; Albrecht, P. Abiotic Oxidation of Petroleum Bitumens under Natural Conditions. *Org. Geochem.* **2000**, *31*, 977−1003.

(7) McConkey, B. J.; Hewitt, L. M.; Dixon, D. G.; Greenberg, B. M. Natural Sunlight Induced Photooxidation of Naphthalene in Aqueous Solution. *Water, Air, Soil Pollut.* **2002**, *136*, 347−359.

(8) Palen, E. J.; Allen, D. T.; Pandis, S. N.; Paulson, S. E.; Seinfeld, J. H.; Flagan, R. C. Fourier transform infrared analysis of aerosol formed in the photo-oxidation of isoprene and β-pinene. *Atmos. Environ. Part A Gen. Top.* **1992**, *26*, 1239−1251.

(9) Aeppli, C.; Swarthout, R. F.; O'Neil, G. W.; Katz, S. D.; Nabi, D.; Ward, C. P.; Nelson, R. K.; Sharpless, C. M.; Reddy, C. M. How Persistent and Bioavailable Are Oxygenated Deepwater Horizon Oil Transformation Products? *Environ. Sci. Technol.* **2018**, *52*, 7250−7258.

(10) Ray, P. Z.; Chen, H.; Podgorski, D. C.; McKenna, A. M.; Tarr, M. A. Sunlight Creates Oxygenated Species in Water-Soluble Fractions of Deepwater Horizon Oil. *J. Hazard. Mater.* **2014**, *280*, 636−643.

(11) Ward, C. P.; Cory, R. M. Assessing the Prevalence, Products, and Pathways of Dissolved Organic Matter Partial Photo-Oxidation in Arctic Surface Waters. *Environ. Sci.: Processes Impacts* **2020**, *22*, 1214−1223.

(12) Ward, C. P.; Sharpless, C. M.; Valentine, D. L.; French-McCay, D. P.; Aeppli, C.; White, H. K.; Rodgers, R. P.; Gosselin, K. M.; Nelson, R. K.; Reddy, C. M. Partial Photochemical Oxidation Was a Dominant Fate of Deepwater Horizon Surface Oil. *Environ. Sci. Technol.* **2018**, *52*, 1797−1805.

(13) Branthaver, J. F.; Huang, S. C. Analytical Separation Methods in Asphalt Research. In *Advances in Asphalt Materials*; Road and Pavement Construction, 2015, pp 31−57. DOI: 10.1016/B978-0-08-100269-8.00002-7.

(14) Mahler, B. J.; Metre, P. C.; Crane, J. L.; Watts, A. W.; Scoggins, M.; Williams, E. S. Coal-Tar-Based Pavement Sealcoat and PAHs: Implications for the Environment, Human Health, and Stormwater Management. *Environ. Sci. Technol.* **2012**, *46*, 3039−3045.

(15) *Evaluations of Carcinogenicity, Overall An Updating of IARC Monographs Volumes 1 to 42*, 1987.

(16) U.S. Department of Health and Human Services. *Report on Carcinogens, Fifteenth Edition*. National Toxicology Program 2021.

(17) *Toxicological Profile for Wood Creosote, Coal Tar Creosote, Coal Tar, Coal Tar Pitch, and Coal Tar Pitch Volatiles*: Atlanta, GA, 2002.

(18) *Monographs on the Evaluation of Carcinogenic Risks to Humans Supplement 7: Coal-Tar Pitches (Group 1)*, 1987.

(19) Mahler, B. J.; Van Metre, P. C.; Bashara, T. J.; Wilson, J. T.; Johns, D. A. Parking Lot Sealcoat: An Unrecognized Source of Urban Polycyclic Aromatic Hydrocarbons. *Environ. Sci. Technol.* **2005**, *39*, 5560−5566.

(20) Van Metre, P. C.; Mahler, B. J. PAH Concentrations in Lake Sediment Decline Following Ban on Coal-Tar-Based Pavement Sealants in Austin, Texas. *Environ. Sci. Technol.* **2014**, *48*, 7222−7228.

(21) Scoggins, M. .; Ennis, T. .; Parker, N. .; Herrington, C. A Photographic Method for Estimating Wear of Coal Tar Sealcoat from Parking Lots. *Environ. Sci. Technol.* **2009**, *43*, 4909−4914.

(22) Watts, A. W.; Ballestero, T. P.; Roseen, R. M.; Houle, J. P. Polycyclic Aromatic Hydrocarbons in Stormwater Runoff from Sealcoated Pavements. *Environ. Sci. Technol.* **2010**, *44*, 8849−8854.

(23) Mahler, B. J.; Van Metre, P. C.; Foreman, W. T. Concentrations of Polycyclic Aromatic Hydrocarbons (PAHs) and Azaarenes in Runoff from Coal-Tar- and Asphalt-Sealcoated Pavement. *Environ. Pollut.* **2014**, *188*, 81−87.

(24) Actions to restrict or discontinue the use of Coal Tar Based Sealants in the United States. https://www.pca.state.mn.us/sites/default/files/tdr-g1-12.pdf (accessed May 10, 2021).

(25) McClintock, N. L.; Turner, M.; Gosselink, L.; Scoggins, M. *PAHs in Austin, Texas Sediments and Coal-Tar Based Pavement Sealants Polycyclic Aromatic Hydrocarbons*; Texas Watershed Protection and Development Review Department: Austin, 2005.

(26) Crane, J.; Grosenheider, K.; Wilson, C. B. *Contamination of Stormwater Pond Sediments by Polycyclic Aromatic Hydrocarbons (PAHs) in Minnesota*; Minnesota Pollution Control Agency: St. Paul, 2010.

(27) Eisler, R. *Polycyclic Aromatic Hydrocarbon Hazards to Fish, Wildlife, and Invertebrates: A Synoptic Review*: Laurelm MD, 1987.

(28) U.S. EPA. *Method 8270E (SW-846): Semivolatile Organic Compounds by Gas Chromatography/Mass Spectrometry (GC/MS)*: Washington DC, 2014.

(29) King, S. M.; Leaf, P. A.; Olson, A. C.; Ray, P. Z.; Tarr, M. A. Photolytic and Photocatalytic Degradation of Surface Oil from the Deepwater Horizon Spill. *Chemosphere* **2014**, *95*, 415−422.
(30) Kaiser, N. K.; Quinn, J. P.; Blakney, G. T.; Hendrickson, C. L.; Marshall, A. G. A Novel 9.4 Tesla FTICR Mass Spectrometer with Improved Sensitivity, Mass Resolution, and Mass Range. *J. Am. Soc. Mass Spectrom.* **2011**, *22*, 1343−1351.
(31) Chacón-Patiño, M. L.; Rowland, S. M.; Rodgers, R. P. Advances in Asphaltene Petroleomics. Part 1: Asphaltenes Are Composed of Abundant Island and Archipelago Structural Motifs. *Energy Fuel.* **2017**, *31*, 13509−13518.
(32) Chacón-Patiño, M. L.; Gray, M. R.; Rüger, C.; Smith, D. F.; Glattke, T. J.; Niles, S. F.; Neumann, A.; Weisbrod, C. R.; Yen, A.; McKenna, A. M.; Giusti, P.; Bouyssiere, B.; Barrère-Mangote, C.; Yarranton, H.; Hendrickson, C. L.; Marshall, A. G.; Rodgers, R. P. Lessons Learned from a Decade-Long Assessment of Asphaltenes by Ultrahigh-Resolution Mass Spectrometry and Implications for Complex Mixture Analysis. *Energy Fuel.* **2021**, *35*, 16335−16376.
(33) Kostyukevich, Y. I.; Vladimirov, G. N.; Nikolaev, E. N. Dynamically Harmonized FT-ICR Cell with Specially Shaped Electrodes for Compensation of Inhomogeneity of the Magnetic Field. Computer Simulations of the Electric Field and Ion Motion Dynamics. *J. Am. Soc. Mass Spectrom.* **2012**, *23*, 2198−2207.
(34) Hendrickson, C. L.; Kaiser, N. K.; Beu, S. C.; Blakney, G. T.; Quinn, J. P.; Smith, D. F.; Marshall, A. G. Characterization of a Modified Dynamically Harmonized FT-ICR Cell at High Magnetic Field. *64th Amer. Soc. Mass Spectrometry Conference on Mass Spectrometry and Allied Topics*: Antonio, TX, 2016.
(35) Blakney, G. T.; Hendrickson, C. L.; Marshall, A. G. Predator Data Station: A Fast Data Acquisition System for Advanced FT-ICR MS Experiments. *Int. J. Mass Spectrom.* **2011**, *306*, 246−252.
(36) Corilo, Y. E. *PetroOrg Software*. Florida State Univsersity, 2013.
(37) Xian, F.; Hendrickson, C. L.; Blakney, G. T.; Beu, S. C.; Marshall, A. G. Automated Broadband Phase Correction of Fourier Transform Ion Cyclotron Resonance Mass Spectra. *Anal. Chem.* **2010**, *82*, 8807−8812.
(38) Kaiser, K. L. E. Correlations of Vibrio Fischeri Bacteria Test Data with Bioassay Data for Other Organisms. *Environ. Health Perspect.* **1998**, *106*, 583−591.
(39) Hughey, C. A.; Hendrickson, C. L.; Rodgers, R. P.; Marshall, A. G.; Qian, K. Kendrick Mass Defect Spectrum: A Compact Visual Analysis for Ultrahigh-Resolution Broadband Mass Spectra. *Anal. Chem.* **2001**, *73*, 4676−4681.
(40) Chacón-Patiño, M. L.; Rowland, S. M.; Rodgers, R. P. The Compositional and Structural Continuum of Petroleum from Light Distillates to Asphaltenes: The Boduszynski Continuum Theory As Revealedby FT-ICR Mass Spectrometry. *The Compositional and Structural Continuum of Petroleum from Light Distillates to Asphaltenes: The Boduszynski Continuum Theory as Revealedby FT-ICR Mass Spectrometry*; ACS Symposium Series, 2018, pp 113−171. DOI: 10.1021/bk-2018-1282.ch006.
(41) McLafferty, F. W.; Turecek, F. Interpretation of Mass Spectra, 4th ed. (McLafferty, Fred W.; Turecek, Frantisek). *Interpretation of Mass Spectra*, 4th ed.; 1994. DOI: 10.1021/ed071pa54.5.
(42) Bowman, D. T.; Jobst, K. J.; Helm, P. A.; Kleywegt, S.; Diamond, M. L. Characterization of Polycyclic Aromatic Compounds in Commercial Pavement Sealcoat Products for Enhanced Source Apportionment. *Environ. Sci. Technol.* **2019**, *53*, 3157−3165.
(43) Thompson, C. J.; Coleman, H. J.; Rall, H. T.; Smith, H. M. Separation of Sulfur Compounds from Petroleum. *Anal. Chem.* **1955**, *27*, 175−185.
(44) Wu, Z.; Jernström, S.; Hughey, C. A.; Rodgers, R. P.; Marshall, A. G. Resolution of 10 000 Compositionally Distinct Components in Polar Coal Extracts by Negative-Ion Electrospray Ionization Fourier Transform Ion Cyclotron Resonance Mass Spectrometry. *Energy Fuel.* **2003**, *17*, 946−953.
(45) Wu, Z.; Rodgers, R. P.; Marshall, A. G. Compositional Determination of Acidic Species in Illinois No. 6 Coal Extracts by Electrospray Ionization Fourier Transform Ion Cyclotron Resonance Mass Spectrometry. *Energy Fuel.* **2004**, *18*, 1424−1428.
(46) Castro-Marcano, F.; Mathews, J. P. Constitution of Illinois No. 6 Argonne Premium Coal: A Review. *Energy Fuel.* **2011**, *25*, 845−853.
(47) Niles, S. F.; Chacón-Patiño, M. L.; Smith, D. F.; Rodgers, R. P.; Marshall, A. G. Comprehensive Compositional and Structural Comparison of Coal and Petroleum Asphaltenes Based on Extrography Fractionation Coupled with Fourier Transform Ion Cyclotron Resonance MS and MS/MS Analysis. *Energy Fuel.* **2020**, *34*, 1492−1505.
(48) Zander, M. On the Nitrogen Containing Constituents of Coal-Tar Pitch. *Fuel* **1991**, *70*, 563−565.
(49) Lopez-avila, V.; Kraska, M.; Flanagan, S. Mass Spectrometric Analysis of Azaarenes in a Coal Tar. *Int. J. Environ. Anal. Chem.* **1988**, *33*, 91−112.
(50) Jones, J. M.; Kubacki, M.; Kubica, K.; Ross, A. B.; Williams, A. Devolatilisation Characteristics of Coal and Biomass Blends. *J. Anal. Appl. Pyrolysis* **2005**, *74*, 502−511.
(51) Sonobe, T.; Worasuwannarak, N.; Pipatmanomai, S. Synergies in Co-Pyrolysis of Thai Lignite and Corncob. *Fuel Process. Technol.* **2008**, *89*, 1371−1378.
(52) Hsu, C. S.; Lobodin, V. V.; Rodgers, R. P.; McKenna, A. M.; Marshall, A. G. Compositional Boundaries for Fossil Hydrocarbons. *Energy Fuel.* **2011**, *25*, 2174−2178.
(53) Lobodin, V. V.; Marshall, A. G.; Hsu, C. S. Compositional Space Boundaries for Organic Compounds. *Anal. Chem.* **2012**, *84*, 3410−3416.
(54) Lin, P.; Fleming, L. T.; Nizkorodov, S. A.; Laskin, J.; Laskin, A. Comprehensive Molecular Characterization of Atmospheric Brown Carbon by High Resolution Mass Spectrometry with Electrospray and Atmospheric Pressure Photoionization. *Anal. Chem.* **2018**, *90*, 12493−12502.
(55) Siegmann, K.; Sattler, K. Formation Mechanism for Polycyclic Aromatic Hydrocarbons in Methane Flames. *J. Chem. Phys.* **2000**, *112*, 698−709.
(56) Chung, S. H.; Violi, A. Peri-Condensed Aromatics with Aliphatic Chains as Key Intermediates for the Nucleation of Aromatic Hydrocarbons. *Proc. Combust. Inst.* **2011**, *33*, 693−700.
(57) EPA Appendix A to 40 CFR, Part 423−126 Priority Pollutants. http://water.epa.gov/scitech/methods/cwa/pollutants.cfm (accessed Mar 30, 2021).
(58) Niles, S. F.; Chacón-Patiño, M. L.; Chen, H.; McKenna, A. M.; Blakney, G. T.; Rodgers, R. P.; Marshall, A. G. Molecular-Level Characterization of Oil-Soluble Ketone/Aldehyde Photo-Oxidation Products by Fourier Transform Ion Cyclotron Resonance Mass Spectrometry Reveals Similarity between Microcosm and Field Samples. *Environ. Sci. Technol.* **2019**, *53*, 6887−6894.
(59) Ruddy, B. M.; Huettel, M.; Kostka, J. E.; Lobodin, V. V.; Bythell, B. J.; McKenna, A. M.; Aeppli, C.; Reddy, C. M.; Nelson, R. K.; Marshall, A. G.; Rodgers, R. P. Targeted Petroleomics: Analytical Investigation of Macondo Well Oil Oxidation Products from Pensacola Beach. *Energy Fuel.* **2014**, *28*, 4043−4050.
(60) Tarr, M. A.; Zito, P.; Overton, E. B.; Olson, G. M.; Adkikari, P. L.; Reddy, C. M. Weathering of Oil Spilled in the Marine Environment. *Oceanography* **2016**, *29*, 126−135.
(61) Kellerman, A. M.; Dittmar, T.; Kothawala, D. N.; Tranvik, L. J. Chemodiversity of Dissolved Organic Matter in Lakes Driven by Climate and Hydrology. *Nat. Commun.* **2014**, *5*, 3804.
(62) Kellerman, A. M.; Kothawala, D. N.; Dittmar, T.; Tranvik, L. J. Persistence of Dissolved Organic Matter in Lakes Related to Its Molecular Characteristics. *Nat. Geosci.* **2015**, *8*, 454−457.
(63) Xu, W.; Gao, Q.; He, C.; Shi, Q.; Hou, Z. Q.; Zhao, H. Z. Using ESI FT-ICR MS to Characterize Dissolved Organic Matter in Salt Lakes with Different Salinity. *Environ. Sci. Technol.* **2020**, *54*, 12929−12937.
(64) Rowland, S. M.; Robbins, W. K.; Corilo, Y. E.; Marshall, A. G.; Rodgers, R. P. Solid-Phase Extraction Fractionation to Extend the Characterization of Naphthenic Acids in Crude Oil by Electrospray

Ionization Fourier Transform Ion Cyclotron Resonance Mass Spectrometry. *Energy Fuel.* **2014**, *28*, 5043−5048.
(65) Lobodin, V. V.; Robbins, W. K.; Lu, J.; Rodgers, R. P. Separation and Characterization of Reactive and Non-Reactive Sulfur in Petroleum and Its Fractions. *Energy Fuel.* **2015**, *29*, 6177−6186.
(66) Ren, L.; Wu, J.; Qian, Q.; Liu, X.; Meng, X.; Zhang, Y.; Shi, Q. Separation and Characterization of Sulfoxides in Crude Oils. *Energy Fuel.* **2019**, *33*, 796−804.
(67) Kabe, T.; Ishihara, A.; Qian, E. W.; Sutrisna, I. P.; Kabe, Y. 3 - Pyrolysis. *Studies in Surface Science and Catalysis*; Elsevier, 2004; Vol. *150*, pp 127−180.
(68) Wang, H.; Dlugogorski, B. Z.; Kennedy, E. M. Analysis of the Mechanism of the Low-Temperature Oxidation of Coal. *Combust. Flame* **2003**, *134*, 107−117.
(69) Zito, P.; Podgorski, D. C.; Johnson, J.; Chen, H.; Rodgers, R. P.; Guillemette, F.; Kellerman, A. M.; Spencer, R. G. M.; Tarr, M. A. Molecular-Level Composition and Acute Toxicity of Photosolubilized Petrogenic Carbon. *Environ. Sci. Technol.* **2019**, *53*, 8235−8243.
(70) Roberts, F. L.; Kandhal, P. S.; Brown, E. R.; Lee, D. Y.; Kennedy, T. W. *Hot Mix Asphalt Materials, Mixture Design, and Construction*; National Asphalt Pavement Association Education Foundation: Lanham, MD, 1996.
(71) Lundstedt, S.; White, P. A.; Lemieux, C. L.; Lynes, K. D.; Lambert, I. B.; Öberg, L.; Haglund, P.; Tysklind, M. Sources, Fate, and Toxic Hazards of Oxygenated Polycyclic Aromatic Hydrocarbons (PAHs) at PAH-Contaminated Sites. *Ambio* **2007**, *36*, 475−485.
(72) Halmi, M. I. E.; Jirangon, H.; Johari, W. L. W.; Abdul Rachman, A. R.; Shukor, M. Y.; Syed, M. A. Comparison of Microtox and Xenoassay Light as a near Real Time River Monitoring Assay for Heavy Metals. *Sci. World J.* **2014**, *2014*, 834202.
(73) Dewhurst, R. E.; Wheeler, J. R.; Chummun, K. S.; Mather, J. D.; Callaghan, A.; Crane, M. The Comparison of Rapid Bioassays for the Assessment of Urban Groundwater Quality. *Chemosphere* **2002**, *47*, 547−554.
(74) Mueller, D. C.; Bonner, J. S.; McDonald, S. J.; Autenrieth, R. L.; Donnelly, K. C.; Lee, K.; Doe, K.; Anderson, J. The Use of Toxicity Bioassays to Monitor the Recovery of Oiled Wetland Sediments. *Environ. Toxicol. Chem.* **2003**, *22*, 1945−1955.

https://doi.org/10.1021/acs.est.2c00582
Environ. Sci. Technol. 2022, 56, 12988−12998